SUPPORTING ONLINE MATERIAL

Giraldez et al. MicroRNAs regulate brain morphogenesis in zebrafish

Materials and Methods

The oligonucleotides used in this study are listed as numbers in the materials and methods. The sequences can be found at the end of the materials and methods.

Germ line replacement

The germ line of embryos from a *dicer*$^{hu715/+}$ intercross was labeled by injecting mRNA for *GFP-nanos3'UTR* at the one cell stage (*1*). Depletion of the host germ line was performed by injection of 3 ng of morpholino antisense oligonucleotide directed against the *dead end* mRNA (*2*). Cells were transplanted from the donors into the host at dome stage. The genotype of the donors was identified by PCR amplification with oligos 27 and 28 and BstBI restriction enzyme digestion. This results in a single band of 175 bp in homozygous *dicer* mutant embryos, two bands of 40 and 135 bp in wild-type embryos, and all three bands in heterozygous. Hosts containing homozygous mutant cells were scored at 30 hpf under a fluorescence microscope to identify successful transfer of germ cells. Fertile adults with a *dicer* mutant germ line have been generated form MZ*dicer* donor embryos, following the procedure described above. At the time this paper was submitted, both male and female adult fish with *dicer* mutant germ lines have been fertile for a year. Mating individual couples has resulted in more than 15 successful crosses per couple, with an average of 100-150 embryos per clutch.

Cloning of mir-1 sequence

DsRed-miR-1[320]: The primers 1 and 2 were used to amplify a 320bp genomic fragment containing the miR-1 precursor and 130bp flanking the hairpin. This PCR product was cloned at the 3' end of the pSP64T+dsRed coding sequence into EcoRI XhoI. dsRed-mir-1[100]: The oligonucleotide pairs 3-5, 4-6 were phosphorylated, annealed and cloned at the 3' end of the pSP64T+dsRed coding sequence in a three-piece ligation to generate dsRed-mir-1[100]. GFP-3xIPT-miR-1: The oligonucleotide pairs 7-8 were phosphorylated, annealed and cloned at the 3' end of pCS2+GFP-F Xho-Xba in a three-piece ligation to generate 3xIPT. This strategy was repeated to generate 6xIPT. GFP-3xPT-miR-#: The oligonucleotides x-y and w-z were phosphorylated, annealed and cloned at the 3' end of pCS2+GFP-F Xho-Xba in a three-piece ligation to generate to generate 3xPT.

miRNA duplexes, mRNA synthesis and injection

mRNA for injection was transcribed using the Message machine kit according to manufacturer's instructions (Ambion). 1000 pl of a 0.2 μg/μl target GFP mRNA solution was injected into wild-type and MZ*dicer* embryos at the one cell stage. ß-Gal control mRNA was co-injected with the target GFP mRNA at 0.1 μg/μl. The miRNA duplexes were purchased from IDT, resuspended in the manufacturer's buffer to a concentration of 100 μM. Working aliquots were prepared in RNase free water at a 10 μM and stored at –80ºC. See below for miRNA:miRNA* sequences. The two most 3' ribonucleotides were replaced by the corresponding deoxynucleotides (i.e. dT). A mismatch was included in the second base of the sense strand of the miRNA to reduce its 5' annealing energy. 500-

1000 pl of a 1-10 μM miRNA duplex solution was injected into wild-type and MZ*dicer* embryos.

Western blot and antibody staining

To analyze GFP expression by Western blot, fourteen embryos were collected 24-30 hours after injection. After removing the yolk, they were homogenized in 40 μl of 1xSDS protein sample buffer and boiled 10 min. 20 μl were loaded per lane in an SDS polyacrylamide gel. The polyacrylamide gel was transferred to a PVDF membrane using a trans-blot semi-dry blotting apparatus (Bio-Rad). The antibodies used for Western blot analysis were mouse anti-actin 1:10000 (Sigma), rabbit anti-ßgal 1:5000 (Molecular Probes) and mouse anti-GFP 1:1000 (Roche). Immunocytochemistry with monoclonal antibodies mouse anti-HNK (1:2000), mouse anti-HuC (1:200), was performed as in (*3*).

Northern blot

Embryos were collected at different stages during development and frozen in liquid nitrogen. Total RNA form thirty embryos was extracted using Trizol (Invitrogen) and resuspended in formamide. Northern blot analysis was performed as described in (*4*).

Northern blots shown in Figure 1 were probed using the starFire oligonucleotide labeling kit and α–P32-ATP (IDT). Other Northern blots were probed using T4 PNK and γ–P32-ATP. For the Northern in Figure S4 and 2C lanes 4 and 5, embryos were collected at 10 hpf. Figure 2C, lanes 1-3: the embryos were genotyped at 24 hpf by tail clipping. After genotyping, the mutant embryos were grouped and the RNA was extracted as indicated above. Twenty micrograms of total RNA per lane were loaded for the Northern shown in

Figure 5. For the Northern blot and miRNA cloning in Figure 5, embryos were collected at the stages: zygote-4 cell, 128-256 cell, germ ring, 75% epiboly, tailbud, 11 somite, 24 hours, and 48 hours.

MicroRNA expression analysis

Total RNA from staged embryos was prepared using Trizol. MicroRNA expression levels were measured by microarray analysis as described in (*13*). Briefly, 5 ug RNA per sample was labeled using T4 RNA ligase and a Cy3 labeled dinucleotide, and hybridized to microarrays that contained probes against the mature sequence of 120 zebrafish microRNAs. An oligonucleotide reference set labeled with Cy5 was included in all hybridizations. Background subtracted Cy3/Cy5 log ratios (base 2) were normalized by a single constant such that the wild type data sets were median centered. This normalization method was used to prevent artificial elevation of the low total signal from MZ*dicer* and Z*dicer* RNA sources. Normalized values were hierarchically clustered using Cluster and the heat map generated using Treeview (Stanford University). Wild-type and Z*dicer* embryos were collected at 28 hpf. MZ*dicer* mutant embryos were collected at 32 hpf to compensate for their developmental delay.

Image acquisition

Embryos were analyzed with Zeiss M2Bio and Axioplan microscopes and photographed with a Zeiss Axiocam digital camera. Embryos in Fig. 3B were photographed and subsequently genotyped. Images were processed with Zeiss AxioVision 3.0.6 and Adobe

Photoshop 7.0 software. For whole mount and flat mounts, different focal planes were merged into a single image using Adobe Photoshop 7.0 software.

Staging of wild-type and MZ*dicer* embryos

MZ*dicer* mutants have a delay of 3-4 hours within the first 24h of development with respect to wild-type embryos. We raised MZ*dicer* at 28ºC and wild-type or Z*dicer* embryos at 22ºC to correct for the developmental delay. Staging was performed according to the number of somites (0-30 hpf) or by time (30-90 hpf). MZ*dicer* survive up to 6 dpf. For the miRNA expression profile wild-type and Z*dicer* embryos were collected at 28 hpf. MZ*dicer* mutant embryos were collected at 32 hpf to compensate for their developmental delay.

Identification of miRNA precursors

Mature miRNA sequences were searched against version 4.0 of the Zebrafish assembly using NCBI BLASTp v2.2.8 (*5*). Those with more than 16 identical nucleotides were parsed. For each miRNA hit to Zebrafish genome two sequences were extracted. The first sequence contained the miRNA match and 60nt of flanking sequence in the 5' direction, while the second sequence contained 60 nt flanking sequence in the 3' direction. These two sequences were analyzed using RNAfold (*6*) to evaluate their potential to form foldback structures. Sequences with less than –20 kcal/mol and with more than 70% of the nucleotides of the miRNA sequence involved in a consistent hairpin structure were selected as candidate miRNA precursor sequences. Each candidate miRNA precursor was then mapped back to the Zebrafish assembly, and if possible to chromosomal coordinates.

A large number of miRNA precursors were located on Scaffold 340 of the assembly that, as yet, has not been mapped to chromosomal coordinates. Precursor structure images were generated using MFOLD (*7*).

Rescue of the MZ*dicer* mutants with miR-430 miRNAs

1000 pl of a 10 μM solution of miR-430a, miR-430b and miR-430c duplexes were injected into MZ*dicer* mutant embryos (see below for the miRNA duplex sequence). The rescue obtained with miR-430a, miR-430b, miR-430c or a combination of all three was equivalent, assayed by ventricle and midbrain-hindbrain boundary formation, and trunk curvature.

Brain labeling using BODIPY Ceramide and Sphingomyelin and TxRed dextran.

Three hours old embryos were incubated for 45 minutes with 200μl of a solution 1:1 mix of BODIPY FL C5-ceramide and BODIPY FL C5-sphingomyelin (1:200 dilution of a 5μg/μl stock; Molecular Probes). One day old embryos were mounted in a thin layer of 0.4% low melting agarose and injected into the midbrain with 1000pl of Texas Red dextran 70,000MW (1:20 dilution of a 500μg/μl stock, Molecular Probes).

Touch sensitivity assay

Wild-type (48h at 22^{o} C) or mutant embryos (48h at 28^{o} C) were touched with a glass needle in the trunk region adjacent to the yolk extension. The response was monitored for three consecutive stimuli. A strong response was characterized by a c-bend opposite to the site of the stimulus. A weak response was characterized as a wiggle of the tail upon

stimulation. No response was recorded after the absence of tail movement upon touching the embryo three times. Different groups of embryos were scored twice.

RT-PCR

Total RNA was extracted from 10 wild-type and MZ*dicer* embryos at 5 hpf. First strand cDNA synthesis was performed according to the manufacturer's instructions using a Retroscript kit (Ambion). PCR was performed using primers 29 and 30, which are present in different exons of the *dicer* gene. Amplification of cDNA results in a 512 bp band. Genomic amplification results in a 920bp band. The primers used to amplify the actin gene were 31 and 32.

Oligonucleotide sequences

These sequences are described 5'-3'. Restriction sites are in lower case, as are nucleotides between miRNA binding sites and those forming mismatches with the miRNA.

dsRed-mir-1[320]

1: ATCGACGATgaattcACACGCTAACCAA

2: CTGGTGAAGTTActcgagGAGCAGCGACT

dsRed-mir-1[100]

3: aattcTGACCTCCTTAGTGTATACATACTTCTTTATGTGCCCATATGAA

4:CATATAAAAGCTATGGAATGTAAAGAAGTATGTATTCTTGGTGAGGTGAc

5:TATATGTTCATATGGGCACATAAAGAAGTATGTATACACTAAGGAGGTCAg

6: tcgagTCACCTCACCAAGAATACATACTTCTTTACATTCCATAGCTTT

3xIPT-miR-1

7:tcgagaatctagaaTACATACTTCTaatCATTCCAtagctaaTACATACTTCTaatCATTCCAt
agctaaTACATACTTCTaatCATTCCAta

8:ctagtaTGGAATGattAGAAGTATGTAttagctaTGGAATGattAGAAGTATGTAttagcta
TGGAATGattAGAAGTATGTAttctagattc

3xPT-miR-1

9:cgagaatctagaaTACATACTTCTTTACATTCCAtagctaaTACATACTTCTTTACATTC
CAtagctaaTACATACTTCTTTACATTCCAta

10:ctagtaTGGAATGTAAAGAAGTATGTAttagctaTGGAATGTAAAGAAGTATGTAtt
agctaTGGAATGTAAAGAAGTATGTAttctagattc

3xPT-17

11x:CTAGctcgagaatctagACTACCTGCACTGTGAGCACTTTGataag

12y:ACTACCTGCACTGTGAGCACTTTGataagACTACCTGCACTGTGAGCACTTT
G

13w:TGCAGGTAGTcttatCAAAGTGCTCACAGTGCAGGTAGTctagattctcgag

14z:TCGACAAAGTGCTCACAGTGCAGGTAGTcttatCAAAGTGCTCACAG

3xPT-204

15x:TAGctcgagaatctagaCAGGCATAGGATGACAAAGGGAAgtcga

16y:CAGGCATAGGATGACAAAGGGAAgtcgaCAGGCATAGGATGACAAAGGGA

Agtc

17w:TCCTATGCCTGtcgacTTCCCTTTGTCATCCTATGCCTGtctagattctcgag

18z:TCGAacTTCCCTTTGTCATCCTATGCCTGtcgacTTCCCTTTGTCA

3xPT-miR-430b

19x:TCGAgaatctagaGTACCCCAACTTGATAGCACTTTtagta

20y:GTACCCCAACTTGATAGCACTTTtagtaGTACCCCAACTTGATAGCACTTTg

21w:CAAGTTGGGGTACtactaAAAGTGCTATCAAGTTGGGGTACtctagattc

22z:CTAGcAAAGTGCTATCAAGTTGGGGTACtactaAAAGTGCTAT

3xPT-miR-430a

23x:TCGAgaatctagaCTACCCCAACAAATAGCACTTAtagta

24y:CTACCCCAACAAATAGCACTTAtagtaCTACCCCAACAAATAGCACTTAg

25w:TTTGTTGGGGTAGtactaTAAGTGCTATTTGTTGGGGTAGtctagattc

26z:CTAGcTAAGTGCTATTTGTTGGGGTAGtactaTAAGTGCTA

Genotyping:

27: AGAAGATGTAAATGTTGAAGACGACCTGGAGTATTATTTCgag

28: CGTCTGGCGAGAAGTGGGAGTTGTG

Dicer RT-PCR

29: ATTCCAATACTTTGGATCT

30: AGTGAAGTCTATAGAGAATGCT

Actin RT-PCR

31: GCCCCACCTGAGCGTAAATA

32: ACAAAAACCCAGACATTGTT

miR-1 duplex

UGGAAUGUAAAGAAGUAUGUAUdTdT

AUACAUACUUCUUUACAUUCGAdTdT

mir-204 duplex

UUCCCUUUGUCAUCCUAUGCCUdGdT

AGGCAUAGGAUGACAAAGGGUAdTdT

mir-430b duplex

AAAGUGCUAUCAAGUUGGGdGdT

CCCAACUUGAUAGCACUAUdTdT

miR-430a duplex

UAAGUGCUAUUUGUUGGGGdTdA

CCCCAACAAAUAGCACUAAdTdT

miR-430c duplex

UAAGUGCUUCUCUUUGGGGdTdA

CCCCAAAGAGAAGCACUAAdTdT

miR-430b-mis

AAAGACCUAUCAAGUUGGGdGdT

CCCAACUUGAUAGGUCUAUdTdT

miR-203 duplex

GUGAAAUGUUUAGGACCACUUdGdT

AAGUGGUCCUAAACAUUUUAGdTdT

Probes:

miR-1: ATACATACTTCTTTACATTCCA

miR-17: ACTACCTGCACTGTAAGCACTTTG

miR-204: CAGGCATAGGATGACAAAGGGAA

miR-430b: GTACCCCAACTTGATAGCACTTT

miR-430a: CTACCCCAACAAATAGCACTTA

miR-26a: AGCCTATCCTGGATTACTTGAA

miR-124a: TTGGCATTCACCGCGTGCCTTA

miR-20: TACCTGCACTATAAGCACTTTA

miR-219: AGAATTGCGTTTGGACAATCA

miR-204: AGGCATAGGATGACAAAGGGAA

Let-7: AACTATACAACCTACTACCTCA

miR-122a: ACAAACACCATTGTCACACTCCA

miR-206: CCACACACTTCCTTACATTCCA

miR-223: GGGGTATTTGACAAACTGACA

miR-17-5p: ACTACCTGCACTGTAAGCACTTTG

5srRNA: TCTCCCATCCAAGTACTAACCAAGCCCGACCCTGCTTA

GFP probe:

Top: TCAAGGACGACGGCAACTACAA

Bottom: CCATGTGATCGCGCTTCTCGTT

Figure S1. Generation of maternal-zygotic *dicer* mutants

(**A**) Protein domains in Dicer. G to U mutation in the *dicer* allele hu715. This mutation in the first RNaseIII domain (*) generates a predicted truncated protein that lacks the RNaseIII catalytic domain and the dsRNA-binding domain (dsRBD) (*9*). (**B**) Schematic representation of the germ line replacement technique used to generate maternal-zygotic *dicer* mutants. Depletion of host germ cells was accomplished by injection of a morpholino (α-PGC-MO) that blocks primordial germ cell (PGC) development in host embryos, resulting in sterility. Donor germ cells labeled with GFP-nos-3'UTR were transplanted into these hosts during early embryogenesis (*2*). Hosts containing *dicer*/*dicer* PGCs were raised to adulthood. These fish only harbored *dicer*/*dicer* PGCs. Intercrossing resulted in embryos that lacked both maternal and zygotic Dicer RNAseIII and dsRBD activity (MZ*dicer*). (**C**) Additional fertile adults were generated using MZ*dicer* embryos as PGC donors. These PGCs gave rise to mature and functional eggs and sperm, which generated embryos with an MZ*dicer* phenotype.

Figure S2. **Maturation and activity of exogenously provided pri-mir-1**

Previous studies have not tested if exogenously provided pri-miRNAs are efficiently processed into mature miRNAs that block target activity in zebrafish. To address this question, we tested processing and silencing activity of pri-miR-1. (**A**) Assay for the processing and activity of pri-miR-1. DsRed-mir-1 contains ß-globin 5' and 3'UTR to stabilize the pri-miRNA, DsRed coding sequence as a fluorescent indicator of translation, and genomic region containing the mir-1 hairpin. GFP-target contains coding sequence of GFP as a fluorescent sensor and three (3x) to six (6x) target sites for miR-1. Targets were

either fully (perfect target) or partially (imperfect target) complementary. DsRed-mir-1 mRNA, GFP-target mRNA and LacZ mRNA were co-injected into 1-cell stage embryos and target expression was analyzed by fluorescent microscopy and Western blot between 24 and 30 hpf. (**B**) To analyze the effect of the flanking genomic regions, we compared the level of expression of mature miR-1 generated by miR-1 hairpin plus 10bp on each side (miR-1[100bp]) or miR-1 hairpin flanked by 130bp of the endogenous genomic sequence on each side (miR-1[320bp]). We observed efficient processing of dsRed-miR-1[320bp] and a strong reduction in the generation of mature miR-1 from dsRed-miR-1[100bp], indicating that information encoded in the region flanking the stem-loop is required for processing. Similar observations have been reported for miR-223 and miR-181 (*8*), but not all pri-miRNAs seem to require the flanking regions for processing (*9-12*). The presence or absence of the coding sequence upstream of the pri-miRNA did not cause significant changes in the processing or expression levels of the mature miR-1 (data not shown). (**C-F**) Silencing activity of dsRed-miR-1[320bp] (C,D) or dsRed-miR-1[100bp] (E,F) analyzed by GFP fluorescence (C,E) and Western blot analysis (D,F) at 24 hpf. Reporters without target sites were not silenced by miR-1 (data not shown). Actin served as a loading control. ß-galactosidase served as an injection control.

Figure S3. Activity of exogenously provided pre-processed miRNA duplexes

To study miRNA-mediated gene silencing by pre-processed miRNAs, we tested the effects of miR-1 and miR-204 on GFP reporters. (**A**) Schematic representation of the experimental set up. GFP-target contains the coding sequence of GFP as a fluorescent sensor and three target sites for miR-1 or miR-204. Targets were either fully (perfect

target) or partially (imperfect target) complementary. miRNA:miRNA* duplexes (miR duplex; miR shown in red) resembled Dicer processing products, with 2-nt 3' overhangs as well as mismatches that were designed to reduce the 5' energy of the sense strand to facilitate its incorporation into the RNA-induced silencing complex (*10*). These miRNA duplexes also resembled siRNA duplexes classically used for gene knock-down experiments in mammalian cells (*11*) in that they were more perfectly paired than typical miRNA duplexes and possessed deoxynucleotides in their 3' overhangs. miR duplexes, GFP-target mRNA and LacZ mRNA were co-injected into 1-cell stage embryos and target cleavage was analyzed by Northern blot (C), and target expression was analyzed by fluorescent microscopy and Western blot between 24 and 30 hpf (B,D,E). (**B**) GFP fluorescence of embryos at 24-30 hpf injected with GFP target mRNA, containing either 3 perfect targets (3xPT) or 3 imperfect targets (3xIPT). Note that miR-1 duplex causes gene silencing of both sensors with perfect and partially complementary target sites. (**C**) Northern blot to visualize GFP mRNA from 15 embryos injected as in (B) four hours after injection. Note the cleavage band induced specifically in embryos that were co-injected with the miRNA duplex and the perfectly complementary target. (**D, E**) Specificity of the gene silencing elicited by miRNA duplexes. Embryos were injected with the indicated sensor mRNAs and the miRNA duplexes. Note that miR-1 specifically silences expression from a sensor containing target sites for miR-1, but does not silence expression from an unrelated target (3xPT-miR-204) and vice versa. (E) Western blot from the embryos shown in panel D probed with anti-GFP antibody to visualize target expression. Actin served as a loading control. ß-galactosidase served as an injection control. Note that co-injection of a miRNA duplex with a sensor with three perfectly

complementary sites results in RNA interference, manifested by sensor silencing and cleavage of the target mRNA. In contrast, co-injection of the miRNA duplex with a sensor with imperfectly complementary targets results in miRNA-like translational inhibition, as manifested sensor silencing but absence of site-specific mRNA target cleavage.

Figure S4. Silencing activity of miRNA duplexes but not pri-miRNAs in maternal-zygotic *dicer* mutants

(**A**) Schematic representation of the experimental set up used. Co-injection of pri-miR (dsRed-miR-1 encoding dsRed and generating miR-1) or miRNA duplexes (miR-1, miR-204, miR-430a or miR-430b) with GFP sensors that contain the coding sequence of GFP and three (3x) or six (6x) imperfect (IPT) or perfect (PT) target sites for the different miRNAs. (**B**) Northern blot analysis of pri-miRNA processing in wild type and MZ*dicer* embryos, showing accumulation of the miR-1 precursor and absence of the mature miRNA in MZ*dicer* mutants. (**C**) Co-injection of GFP sensors with buffer (–), dsRed-mir-1 or miR-1 duplexes into wild type or MZ*dicer* mutants. Fluorescent microscopy shows GFP target expression (green) or dsRed-mir-1 expression (red) at 24-30 hpf. Bright field image of embryos is shown below. (**D, E**) Western blot to detect target GFP expression from the embryos co-injected with GFP sensors and buffer (–), dsRed-mir-1 or miR duplexes into wild type or MZ*dicer* mutants. Actin was used as a loading control. Note that pri-mir-1 or endogenous pri-mir-430 are active in wild type but do not repress sensor expression in MZ*dicer* mutants. However, miRNA duplexes elicit specific silencing of their corresponding targets in wild type and MZ*dicer* mutant embryos.

Figure S4. Morphogenesis defects in maternal-zygotic *dicer* mutants

DIC images of 24 hpf wild-type and MZ*dicer* embryos. Lateral (**A**, **A'**) and dorsal (**B**, **B'**, **C**, **C'**) view of the brain. Note the malformation of the retina, the absence of the midbrain-hindbrain boundary (**B**, **B'**, arrow) and constrictions in the hindbrain (**C**, **C'**, bracket). MZ*dicer* fail to form ventricles in the head region (**B**, **B'** arrowhead). Lateral view of the somites (**D**, **D'**, **E**, **E'**, **F**, **F'**). MZ*dicer* embryos exhibit a reduced floor plate (**E'**, bracket) and abnormal somite boundaries and morphology (**F'**, <).

Figure S6. Neural patterning in maternal-zygotic *dicer* mutants

To investigate whether the morphogenetic defects observed in MZ*dicer* mutants were the result of a defective neural plate patterning, we analyzed anterior-posterior and dorsal-ventral regionalization using in situ hybridization. Wild-type and MZ*dicer* embryos at the 14-somite stage. Expression of the anterior-posterior markers *pax2a* (**A, A'**), and *emx1*, *eng2* and *krox20* (**B, B'**). Expression of the dorsal-ventral markers, *odd paired like* (*opl*, **C, C'**, in the dorsal neural tube) and *sonic hedgehog* (*shh*, **D, D'** ventral neural tube). Note the normal specification of optic stalk (*pax2a*), forebrain (*emx1*, *opl*), midbrain-hindbrain boundary (*eng2* and *pax2a*), otic vesicles (*pax2a*) and hindbrain rhombomeres (*krox20*). os, optic stalk/anterior retina; te, telencephalon; vd, ventral diencephalon; vm, ventral midbrain; MHB, midbrain-hindbrain boundary; r3, r5, rhombomeres 3 and 5; ov, otic vesicle; n, notochord; pd, pronephric duct.

Figure S7. Neuronal differentiation in maternal-zygotic *dicer* mutants

To investigate the role of mature miRNAs during neuronal differentiation and axonal projection we performed inmunostainings with HNK-1 (axons) and HuC (neuronal cell bodies) antibodies in wild type (**A**), MZ*dicer* mutants (**B**) and MZ*dicer*$^{+miR\text{-}430}$ (**C**). (B) MZ*dicer* mutants have ectopically located trigeminal neurons (arrowhead). Fasciculation of the axons in the hindbrain (red bracket) and the postoptic commissure (arrow) is reduced. (C) MZ*dicer*$^{+miR\text{-}430}$ have a reduced number of ectopic trigeminal neurons (arrowhead) and a partial rescue of the fasciculation defects (red bracket).

Figure S8. Touch-induced escape response in maternal-zygotic *dicer* mutants

As a behavioral assay, the escape response induced by touch was analyzed. At about 48h of development, wild-type embryos respond to touch with a movement of the tail contra-lateral to where the stimulus is applied, generating a characteristic c-bend (12). (**A-C**) Single frames from a video showing the touch response of wild-type, MZ*dicer* and MZ*dicer*$^{+miR\text{-}430}$ embryos. Note the c-bend contra-lateral to where the stimulus is applied in wild type and MZ*dicer*$^{+\text{miR-}430}$ (double arrow) but not MZ*dicer*. (**D**) The touch response was classified as strong, weak, or no response (see Material and methods). MZ*dicer* embryos are almost immotile and fail to respond to touch (32%) or produce a small twitch of the tail (weak, 68%, n=58). Only 8% of the MZ*dicer* embryos showed a significant movement of the tail upon stimulation. MZ*dicer*$^{+miR\text{-}430}$ embryos elicited a strong response in 72% of the embryos (n=109).

Figure S9. Hematopoietic, endothelial and muscle marker expression in maternal-zygotic *dicer* mutants

(**A-B'**) Lateral view (left) and dorsal view (middle and right); (**A, A'**) stem cell leukemia (*scl*, arrowhead) and *fgf8* (*) mRNA expression in wild-type and MZ*dicer* embryos. (**B, B'**) *fli-1* mRNA expression in wild-type and MZ*dicer* embryos. Note the reduction of endothelial *fli-1* expression. Anterior is to the left. (**C-C'**) Dorsal view of a whole mount (left) and a flat mount (middle and right) of embryos labeled with the muscle marker *myoD*, indicating muscle precursor differentiation in wild type and MZ*dicer* mutants.

Figure S10. Ear and heart morphogenesis defects in maternal-zygotic *dicer* mutants

To investigate the role of Dicer and miRNAs during organogenesis, we examined the ear and the heart morphogenesis in wild-type and MZ*dicer* embryos at 72 hpf. MZ*dicer* embryos fail to form otoliths in the ear (arrowheads) and lack clearly separated atrial and ventricular chambers, forming a tubular structure (arrow).

Figure S11. Rescue of maternal-zygotic *dicer* mutants by miRNA duplexes

To address the specificity of the rescue of MZ*dicer* mutant embryos elicited by miR-430 and a possible functional redundancy among different members of the miR-430 family, we tested the rescue capabilities of individual miR-430 family members and compared them with a combination of three different members, unrelated miRNA duplexes and a miR-430 duplex including two mismatch in the seed region. Lateral views of MZ*dicer* mutant embryos (36 hpf) injected with miRNA duplexes. Co-injection of a combination

of miR-430a, miR-430b and miR-430c duplexes rescues to the same extent as each individual miRNA duplex alone. Injection of a mismatch miRNA duplex (miR-430b-mis) or of an unrelated miRNA duplex (miR-203) does not result in any rescue (n>30).

References

1. M. Koprunner, C. Thisse, B. Thisse, E. Raz, *Genes Dev* **15**, 2877-85 (Nov 1, 2001).
2. B. Ciruna *et al*., *Proc Natl Acad Sci U S A* **99**, 14919-24 (Nov 12, 2002).
3. A. F. Schier *et al.*, *Development* **123**, 165-78 (Dec, 1996).
4. R. C. Lee, V. Ambros, *Science* **294**, 862-4 (Oct 26, 2001).
5. S. F. Altschul *et al.*, *Nucleic Acids Res* **25**, 3389-402 (Sep 1, 1997).
6. S. Wuchty, W. Fontana, I. L. Hofacker, P. Schuster, *Biopolymers* **49**, 145-65 (Feb, 1999).
7. M. Zuker, *Nucleic Acids Res* **31**, 3406-15 (Jul 1, 2003).
8. C. Z. Chen, L. Li, H. F. Lodish, D. P. Bartel, *Science* **303**, 83-6 (Jan 2, 2004).
9. E. Wienholds, M. J. Koudijs, F. J. van Eeden, E. Cuppen, R. H. Plasterk, *Nat Genet* **35**, 217-8 (2003).
10. D. S. Schwarz *et al.*, *Cell* **115**, 199-208 (Oct 17, 2003).
11. S. M. Elbashir *et al.*, *Nature* **411**, 494-8 (May 24, 2001).
12. M. Granato *et al*., *Development* **123**, 399-413 (Dec, 1996).
13. J. M. Thomson, J. Parker, C. M. Perou, S. M. Hammond, *Nat Methods* **1**, 47-53 (2004).

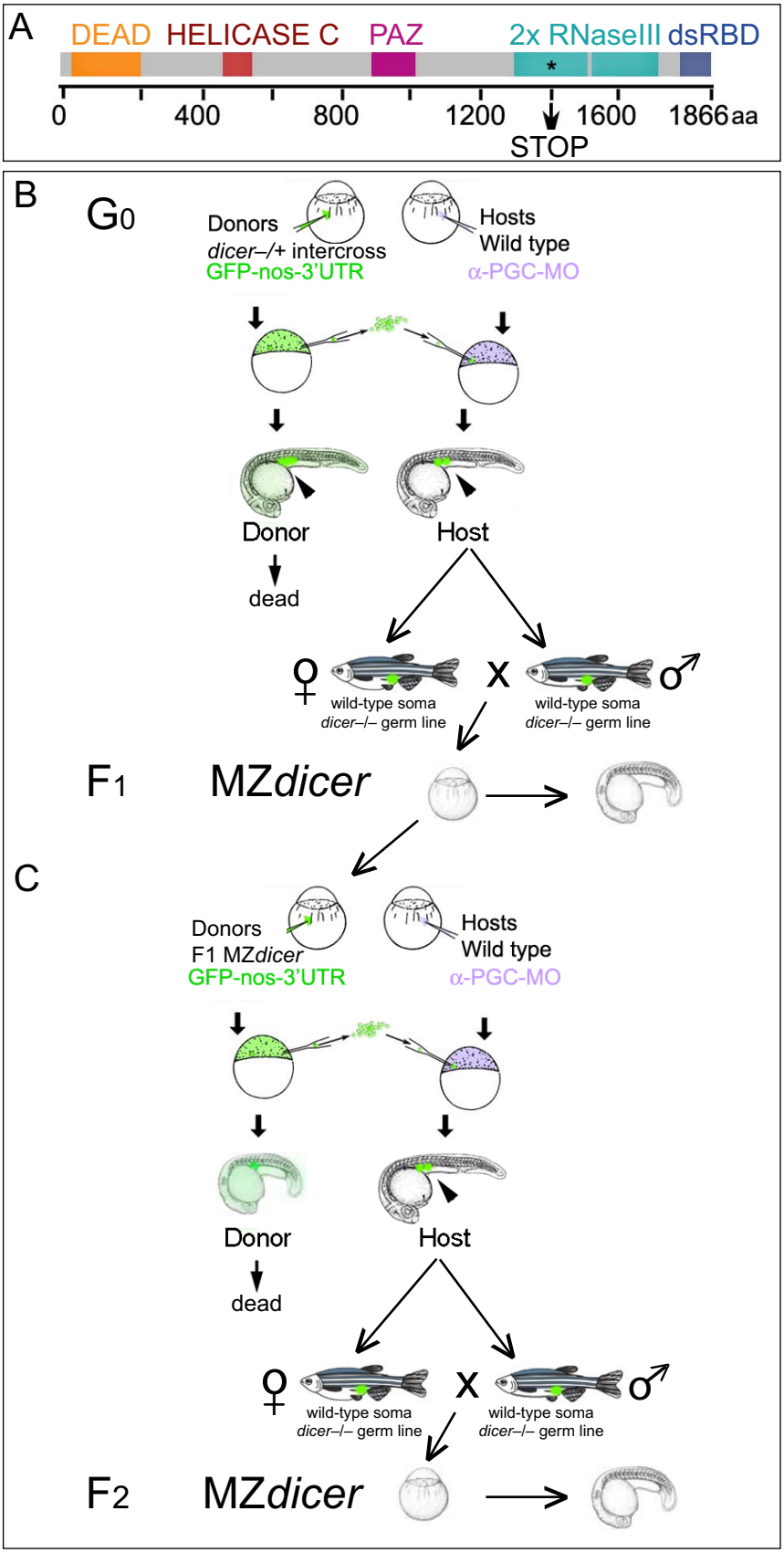

Giraldez et. al., Supp Figure 1

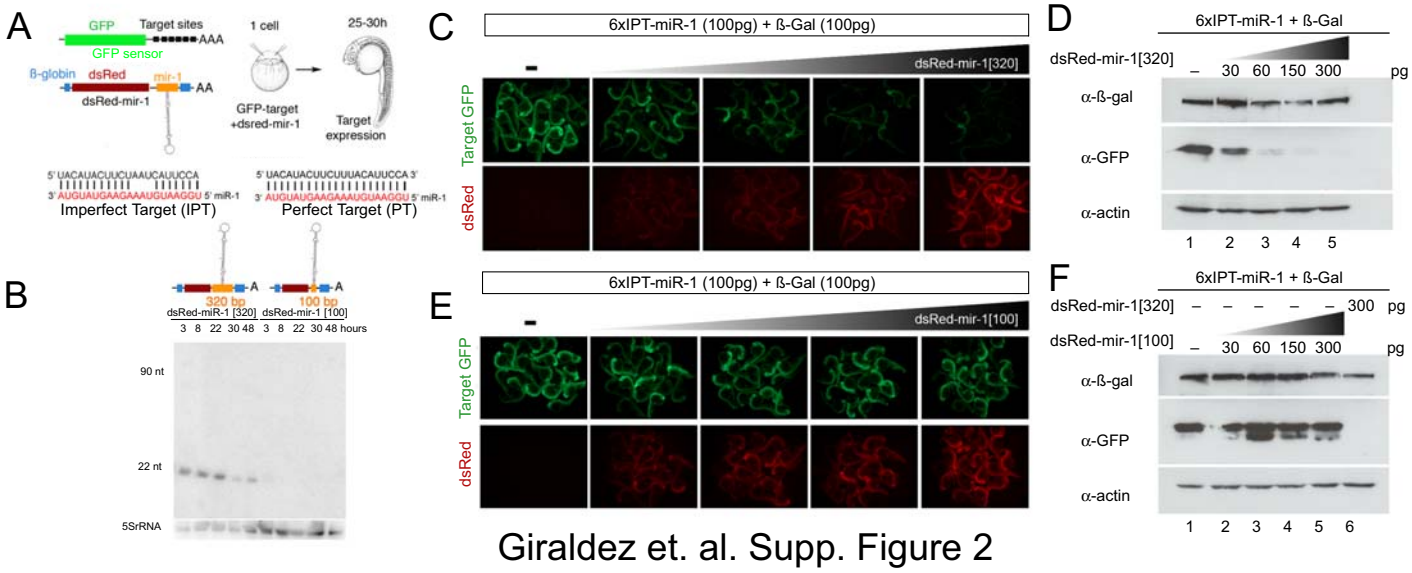

Giraldez et. al. Supp. Figure 2

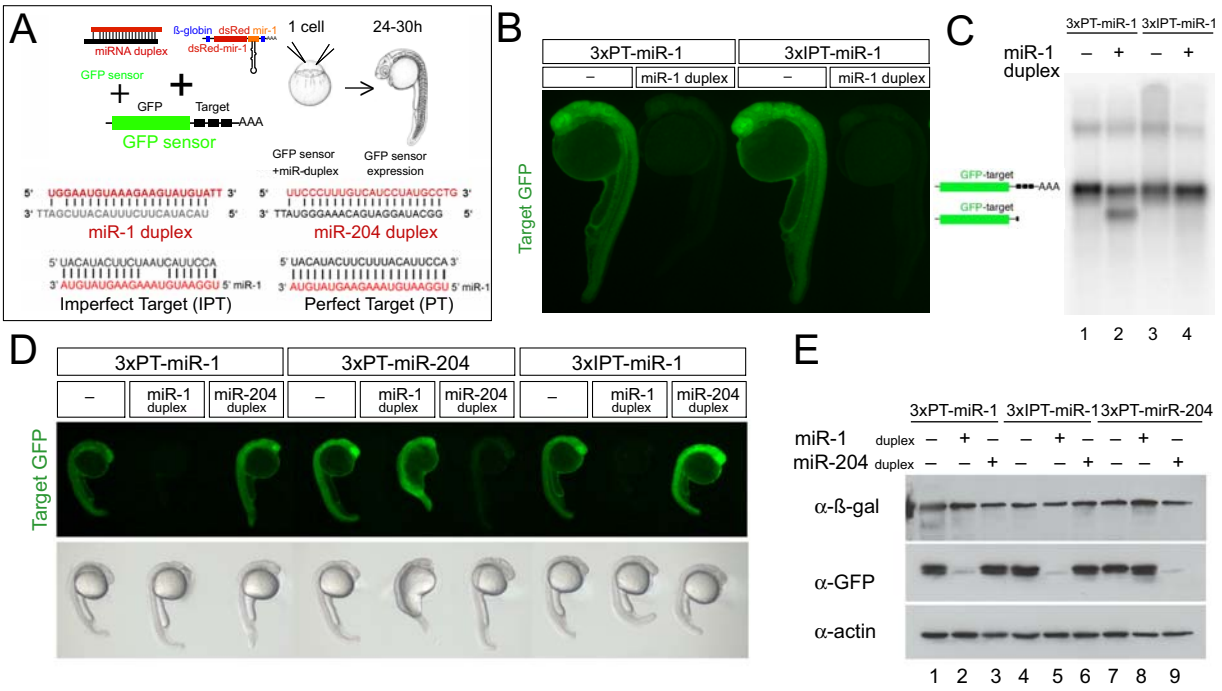

Giraldez et. al.Supp. Figure 3

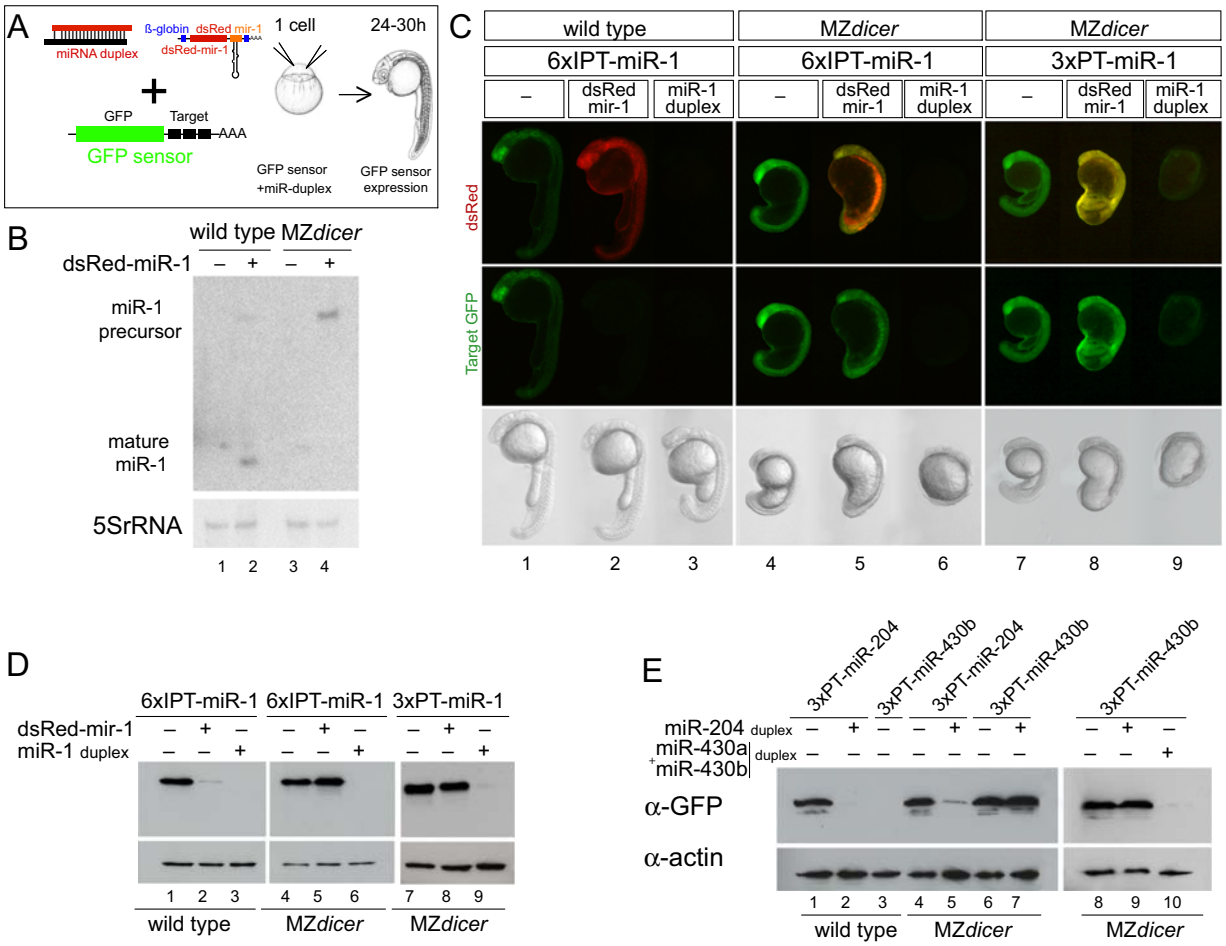

Giraldez et. al. Supp. Figure 4

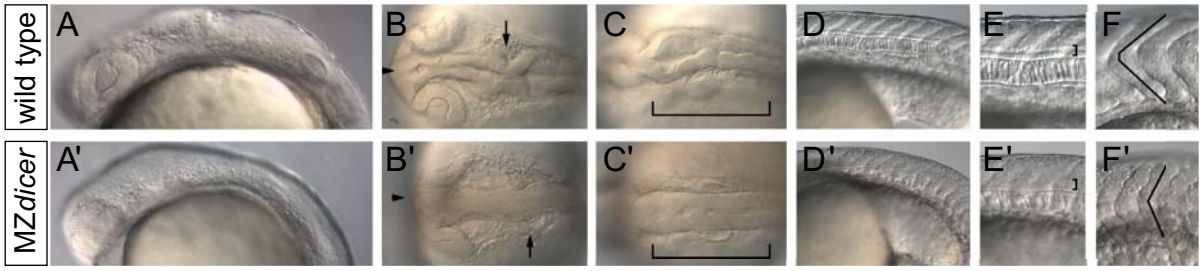

Giraldez et. al. Supp Figure 5

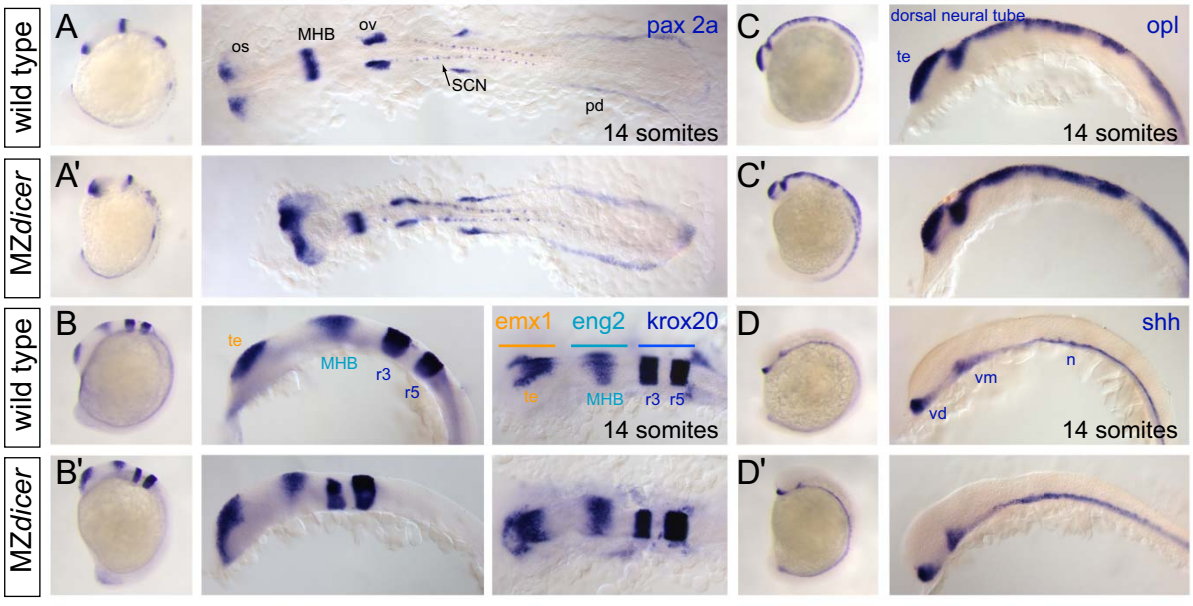

Giraldez et. al. Supp. Figure 6

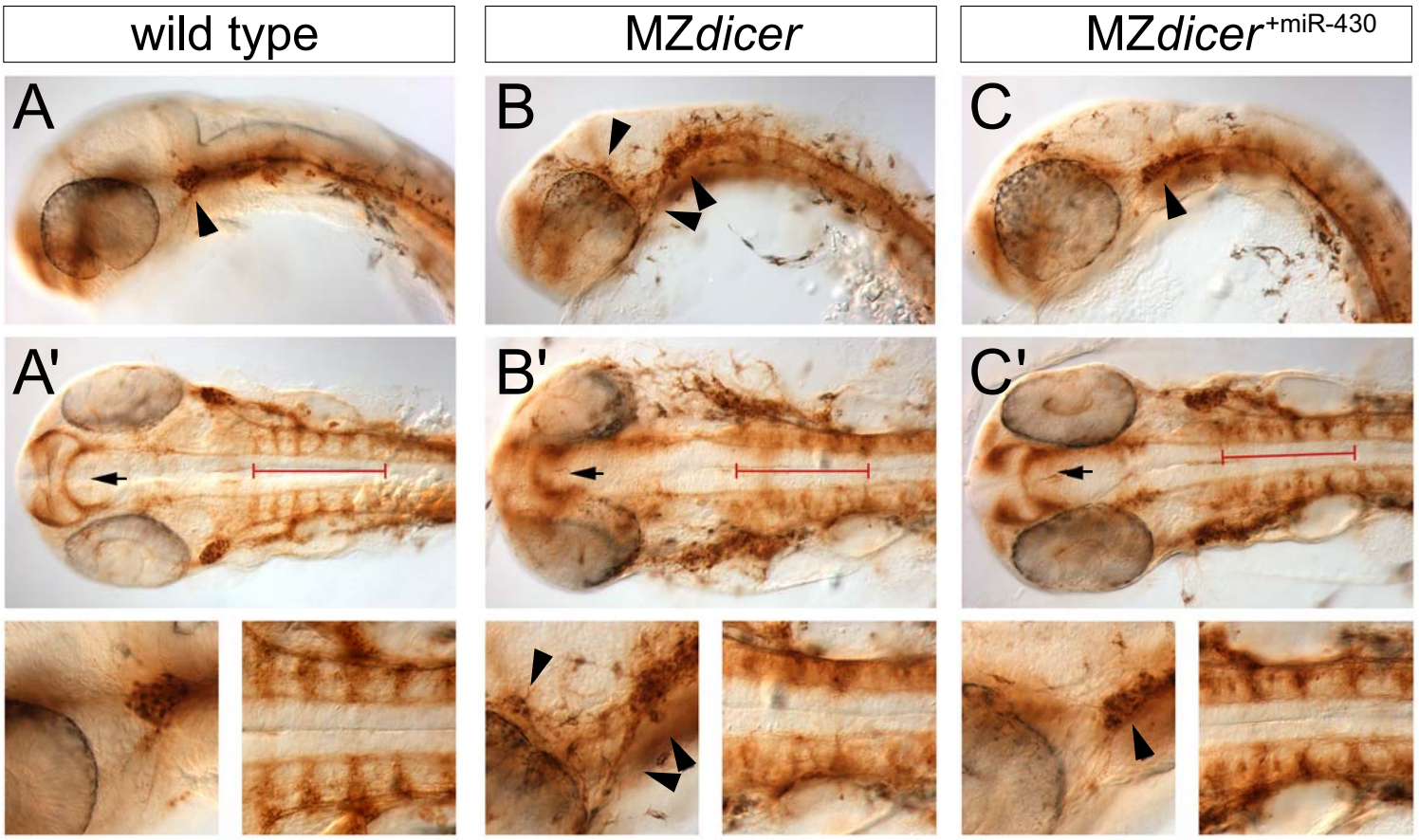

Giraldez et. al. Supp. Figure 7

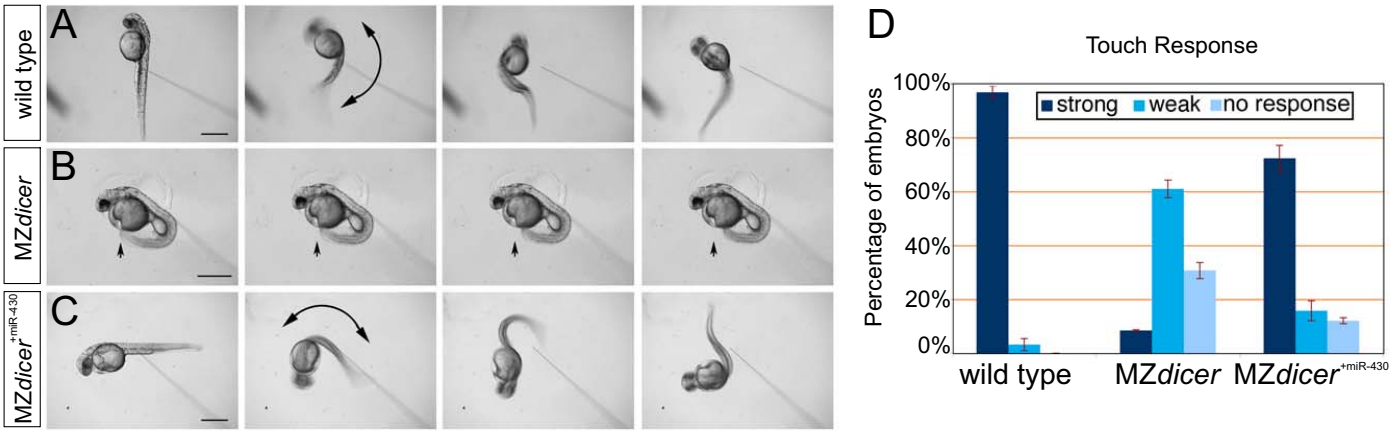

Giraldez et. al. Supp Figure 8

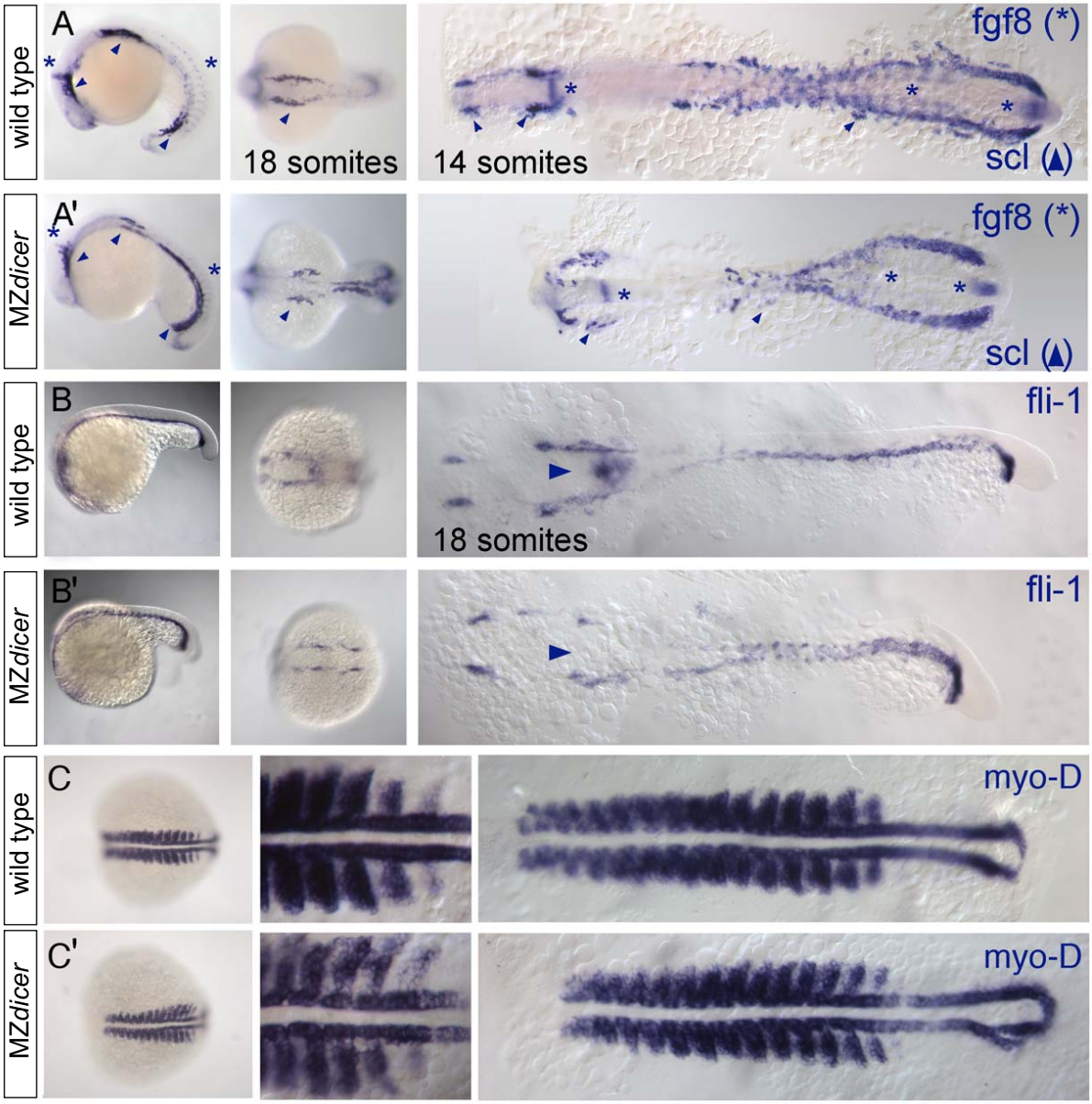

Giraldez et. al. Supp. Figure 9

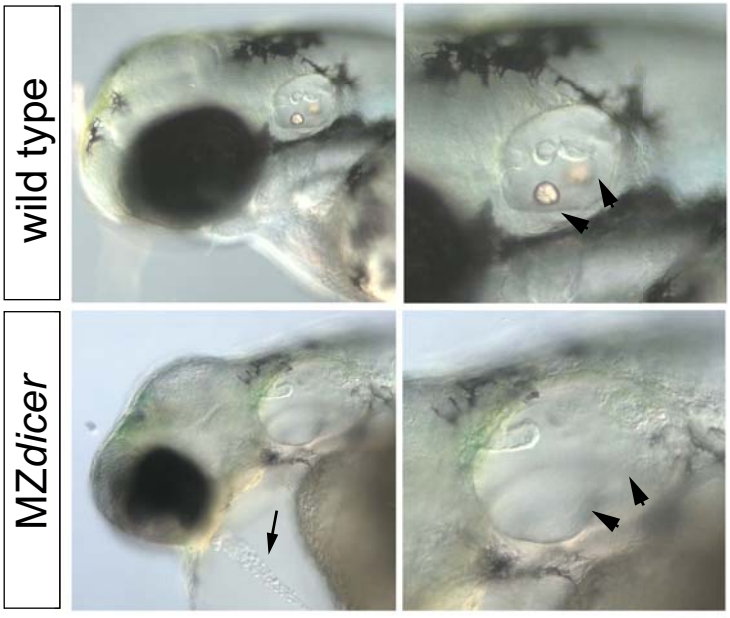

Giraldez et. al. Supp. Figure 10

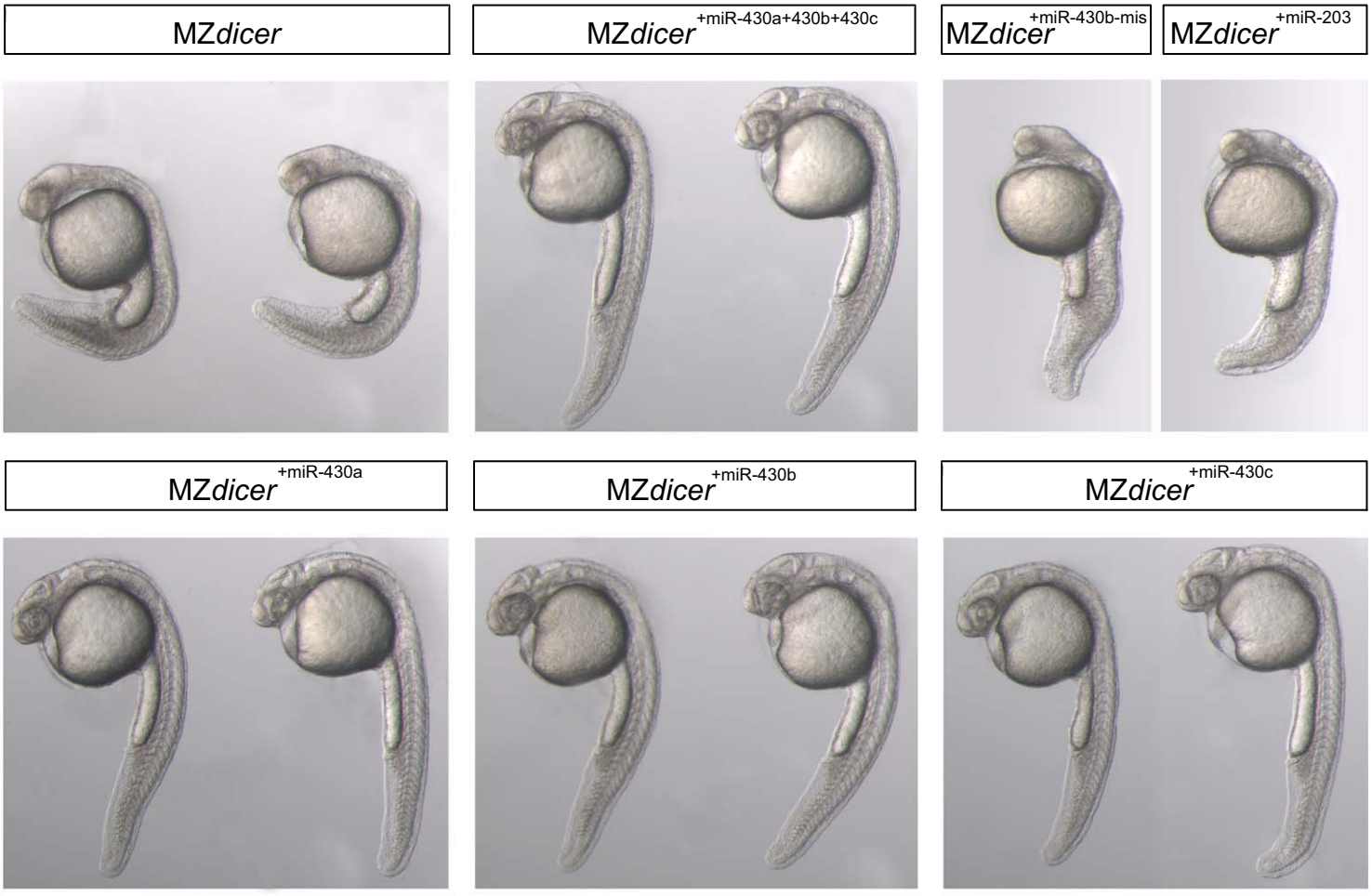

Giraldez et. al.Supp. Figure 11